

10^4) (14), the spectral positions of the MDR's oscillate as well. The observed oscillation frequency and damping constant for the resonance peak positions have been used to determine the dynamic surface tension and viscosity for flowing droplets (13).

The occurrence of the red laser emission at the spherical liquid-air boundary (Fig. 2) clearly demonstrates that optical feedback is confined near the surface, confirming the surface nature of the output resonance. As discussed earlier, the broadband fluorescence emission of the laser dye ensures that some of the wavelengths within the fluorescence bandwidth will satisfy resonance conditions for any droplet morphology, and it will be at those wavelengths that enhanced optical feedback occurs. It is the optical feedback at these different specific wavelengths that gives rise to the lasing surface wave. In contrast, the two green spots located on the front and back surfaces of the droplet (Fig. 2) result from the specular reflections of incident radiation at the interface. When the input resonance condition is fulfilled, other parts of the droplet interface in addition to the two spots will exhibit green radiation (4). However, since the incident laser radiation is monochromatic, the input resonance condition can be satisfied only for specific droplet sizes and shapes. In contrast, since the laser emission

is broadband, the output resonance condition can always be satisfied for all sizes and shapes, as Figs. 2 and 3 indicate.

The surface-wave nature of the laser emission provides a novel means for observing droplets of different sizes and shapes and particularly for highlighting their liquid-air interface. Photographs of a droplet stream within the first few millimeters of the orifice exit are shown in Fig. 3. The droplets are generated from a cylindrical stream of liquid that is periodically pinched off by the vibrating orifice. The highly distorted droplets evolve into more regular and discrete spheroids that undergo a series of shape oscillations, becoming alternately prolate and oblate. Farther downstream from the orifice, surface tension forces the droplets to become essentially spherical (Fig. 2). The details of the evolution from a cylindrical stream to spherical droplets, particularly the interfacial regions, are highlighted by laser emission from all irradiated portions of the droplet stream. As seen in Fig. 3, it is clearly not necessary that the droplets be spherical or of a particular size for laser emission to be achieved. Laser emission is also present in the much smaller satellite droplets and in the cylindrical necking regions of the droplet stream (Fig. 3).

Regardless of the highly distorted droplet shape and size, near-field photographs dem-

onstrate that laser emission highlights the liquid-air interface. Such laser emission photographs can provide a novel technique to study droplet dynamics.

REFERENCES AND NOTES

1. A. Ashkin and J. M. Dziedzic, *Appl. Opt.* **20**, 1803 (1981); J. F. Owen, P. W. Barber, B. J. Messinger, R. K. Chang, *Opt. Lett.* **6**, 272 (1981).
2. R. E. Benner, P. W. Barber, J. F. Owen, R. K. Chang, *Phys. Rev. Lett.* **44**, 475 (1980).
3. J. F. Owen, R. K. Chang, P. W. Barber, *Aerosol Sci. Technol.* **1**, 293 (1982); R. Thurn and W. Kiefer, *Appl. Spectrosc.* **38**, 78 (1984).
4. A. Ashkin, *Science* **210**, 1081 (1980).
5. M. Kerker, *The Scattering of Light and Other Electromagnetic Radiation* (Academic Press, New York, 1969); C. F. Bohren and D. R. Huffman, *Absorption and Scattering of Light by Small Particles* (Wiley, New York, 1983).
6. J. F. Owen, R. K. Chang, P. W. Barber, *Opt. Lett.* **6**, 540 (1981).
7. A. B. Pluchino, *Appl. Opt.* **20**, 2986 (1981).
8. J. B. Snow, S.-X. Qian, R. K. Chang, *Opt. Lett.* **10**, 37 (1985).
9. H.-M. Tzeng, K. F. Wall, M. B. Long, R. K. Chang, *ibid.* **9**, 499 (1984).
10. H.-M. Tzeng, K. F. Wall, M. B. Long, R. K. Chang, *ibid.*, p. 273.
11. P. Chýlek, J. T. Kiehl, M. K. W. Ko, *Appl. Opt.* **17**, 3019 (1978).
12. A. Ashkin and J. M. Dziedzic, *Phys. Rev. Lett.* **38**, 1351 (1977).
13. H.-M. Tzeng, M. B. Long, R. K. Chang, P. W. Barber, *Opt. Lett.* **10**, 209 (1985).
14. H. Lamb, *Hydrodynamics* (Dover, New York, 1945), pp. 475 and 639.
15. Supported in part by the Air Force Office of Scientific Research (contract F49620-85-K-0002) and the Army Research Office (contract DAAG29-85-K-0063).

21 June 1985; accepted 30 September 1985

Indirect Observation by ^{13}C NMR Spectroscopy of a Novel CO_2 Fixation Pathway in Methanogens

JEREMY N. S. EVANS, CYNTHIA J. TOLMAN, MARY F. ROBERTS

High-field carbon-13 nuclear magnetic resonance (NMR) spectroscopy has been used to monitor the isotopic dilution of doubly carbon-13-labeled precursors for 2,3-cyclopyrophosphoglycerate, a novel primary metabolite that occurs in certain methanogens. A unique carbon dioxide fixation pathway that gives rise to asymmetric labeling of acetyl coenzyme A has been demonstrated in *Methanobacterium thermoautotrophicum*. The effect of selected metabolic inhibitors on the labeled species in the pathway has been examined by NMR. These techniques establish a general, sensitive method for the delineation of convergent biosynthetic pathways.

METHANOGENS ARE ARCHAEABACTERIA (1) that can produce methane by reduction of carbon dioxide with hydrogen. This reaction provides the cells with energy. The fixation of CO_2 , which is the sole carbon source for autotrophic methanogens, into cellular material initially occurs by formation of acetyl coenzyme A (CoA) (2-4), and this has been shown (4, 5) to be derived from CO_2 via two different pathways. Neither the Calvin cycle (6) nor the reductive tricarboxylic acid

cycle (7) operates in CO_2 assimilation in the methanogenic autotroph *Methanobacterium thermoautotrophicum* (2, 8, 9). Instead, carbon assimilation takes place by a third CO_2 fixation pathway, in which 90 percent of the total CO_2 is converted into CH_4 and the remainder is used largely for acetyl CoA synthesis (10). The novel metabolite 2,3-cyclopyrophosphoglycerate (CPP) is formed rapidly at high intracellular concentrations (10 mM) (11). Recent carbon-13 (^{13}C) nuclear magnetic resonance (NMR) studies

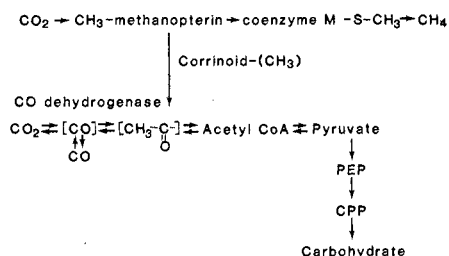
have shown that CO_2 , acetate, pyruvate, and phosphoenolpyruvate (PEP) serve as biosynthetic precursors for CPP and that CPP occupies a central role in carbohydrate metabolism (12).

Methanobacterium thermoautotrophicum cells fed with $^{13}\text{CO}_2$ exhibit intense resonances at 70.1 and 78.6 parts per million (ppm); these peaks were assigned to C-3 and C-2 of CPP (11). Furthermore, [^{13}C]acetate is incorporated specifically into C-2 of CPP, [^{13}C]acetate into C-3 of CPP, and [^{13}C]pyruvate into C-1 of CPP. Since CPP is rapidly and intensely labeled by $^{13}\text{CO}_2$, [^{13}C]acetate, and [^{13}C]pyruvate, it is a suitable probe for reactions leading up to C₃ units. In particular, with the use of doubly labeled precursors, ^{13}C NMR can be employed to detect any scrambling of C₂ or C₃ units that occurs in *Mb. thermoautotrophicum*. The spin-spin coupling (J_{CC}) of [^{13}C]CPP is thus diagnostic for the integrity of a C₂ precursor such as [^{13}C]acetate. If label scrambling were to

Department of Chemistry, Massachusetts Institute of Technology, Cambridge 02139.

occur, the C₂ unit would be degraded to C₁ units, which can exchange with ¹²CO₂, resulting in the introduction of ¹²C next to ¹³C on resynthesis. That scrambling of CPP can take place after its formation can be ruled out, since the forward reaction from CPP leads to gluconeogenesis, and the back reaction from CPP to PEP or pyruvate is disfavored thermodynamically (12).

Feeding experiments with [1,2-¹³C₂]acetate and [2,3-¹³C₂]pyruvate show that scrambling of the ¹³C-¹³C unit does indeed occur (Fig. 1). The C-2 of CPP labeled from [1,2-¹³C₂]acetate appears as a double doublet (¹J_{CC} = 39.0 Hz, ²J_{CP} = 6.3 Hz) with a relatively small superimposed central doublet (²J_{CP} = 6.2 Hz) (Fig. 1B). The latter central peak arises from ¹³C next to ¹²C. The C-3 of CPP shows more total ¹³C intensity and exhibits a more intense central doublet (²J_{CP} = 7.1 Hz) flanked by a double doublet. The large central doublet for C-3 reflects the greater amount of ¹²C at C-2 of CPP. This labeling pattern can be rationalized in terms of the asymmetric acetic acid pathway shown in scheme 1.



Carbon monoxide dehydrogenase has been extensively studied (13, 14) from the acetogen *Clostridium thermoaceticum* and is thought to fix one CO₂, which gives rise to the carboxylate of acetate (15). That the enzyme carries out the reduction of CO₂ in the presence of hydrogen, to yield enzyme-bound CO, is borne out by recent observations of CO formation accompanying methanogenesis (5, 16, 17). The novel C₁-methanopterin (18) involved in methanogenesis also acts as the precursor for the methyl carbon of acetate. Our ¹³C NMR data indicate that [¹³C₂]acetate or its activated form can be broken down to an activated [¹³C]methyl derivative and bound ¹³CO. Only the latter exchanges appreciably with the ¹²CO₂ pool, presumably via carbon monoxide dehydrogenase.

A comparison of ¹³C coupling patterns for CPP incubated with [1,2-¹³C₂]acetate for 6 and 12 hours reveals little change in the isotopic dilution pattern, although the total ¹³C intensity is increased. The CPP pool is dynamic, and its turnover rate is regulated by the cell growth rate (12). The invariability in the J_{CC} patterns must reflect an equilibrium of back flux of acetate

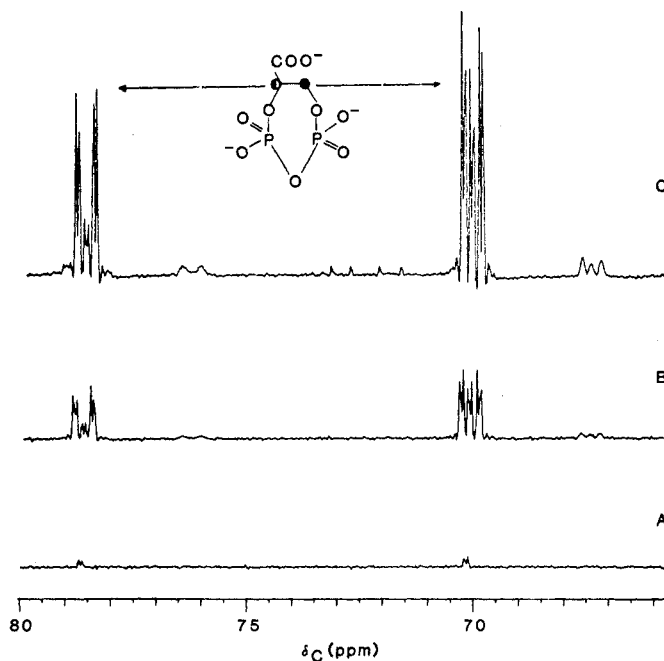


Fig. 1. ¹H-decoupled ¹³C NMR spectra (100.6 MHz) of ethanol extracts of *Mb. thermoautotrophicum* fed for 6 hours with (A) ¹²CO₂/H₂ (1:4 by volume); (B) ¹²CO₂/H₂ (1:4 by volume) plus [1,2-¹³C₂]acetate (20 mM); and (C) ¹²CO₂/H₂ (1:4 by volume) plus [2,3-¹³C₂]pyruvate (10 mM). Spectral intensities in (A) and (B) are normalized to those in (C). Cells of *Mb. thermoautotrophicum* were grown and extracted as described (11), and ¹³C feeding experiments were performed as described (12). NMR spectra were obtained with a flip angle of 90°, a recycle time of 1 second, and a spectral resolution of 1.53 Hz per point.

through C₁ units and forward flux to CPP. The incorporation of [2,3-¹³C₂]pyruvate into CPP shows the same behavior as [1,2-¹³C₂]acetate except that more ¹³C is incorporated into CPP overall (Fig. 1C). This is consistent with pyruvate being a later biosynthetic precursor for CPP than acetate. The scrambling exhibited by the [2,3-¹³C₂]pyruvate feeding experiment also establishes the reversibility of pyruvate synthase, the enzyme that condenses activated acetic acid and CO₂.

As an extension to the use of doubly labeled precursors for CPP to probe C₁ → C₂ reactions, we investigated the effect of selected metabolic inhibitors on [¹³C₂]acetate incorporation. The effect of cyanide and propyl iodide on CPP synthesis from [1,2-¹³C₂]acetate was assessed in *Mb. thermoautotrophicum*. Since cyanide is known to inhibit CO dehydrogenase (19), it should prevent bound ¹³CO, generated by the [¹³C₂]acetate back reaction of acetate synthesis, from exchanging with ¹²CO₂. As predicted, cells fed on [1,2-¹³C₂]acetate, ¹²CO₂/H₂, and KCN (50 μM) showed rapid labeling of CPP (Fig. 2B) but no scrambling (that is, no significant ¹³C central doublet above natural abundance levels for C-3 of CPP).

Propyl iodide, at concentrations up to 50 μM, inhibits the growth of *Mb. thermoautotrophicum* (20) and is thought to inhibit the formation of a methylated corrinoid enzyme (21) that is probably involved in acetate synthesis (17). It therefore prevents the formation of the methyl group of acetate from

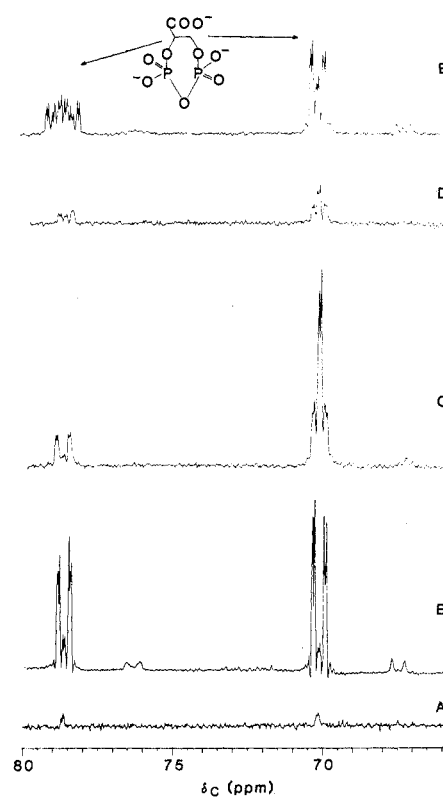


Fig. 2. ¹H-decoupled ¹³C NMR spectra (100.6 MHz) of ethanol extracts of *Mb. thermoautotrophicum* fed for 6 hours with [1,2-¹³C₂]acetate (20 mM), ¹²CO₂/H₂ (1:4 by volume), and (A) no additions (control); (B) cyanide (50 μM); (C) propyl iodide (100 μM); and (D) fluoropyruvate (1 mM). In (E) cells were fed with ¹³CO₂/H₂ (1:4 by volume) plus fluoropyruvate (1 mM) for 2 hours. Spectra were obtained with the parameters outlined in Fig. 1.

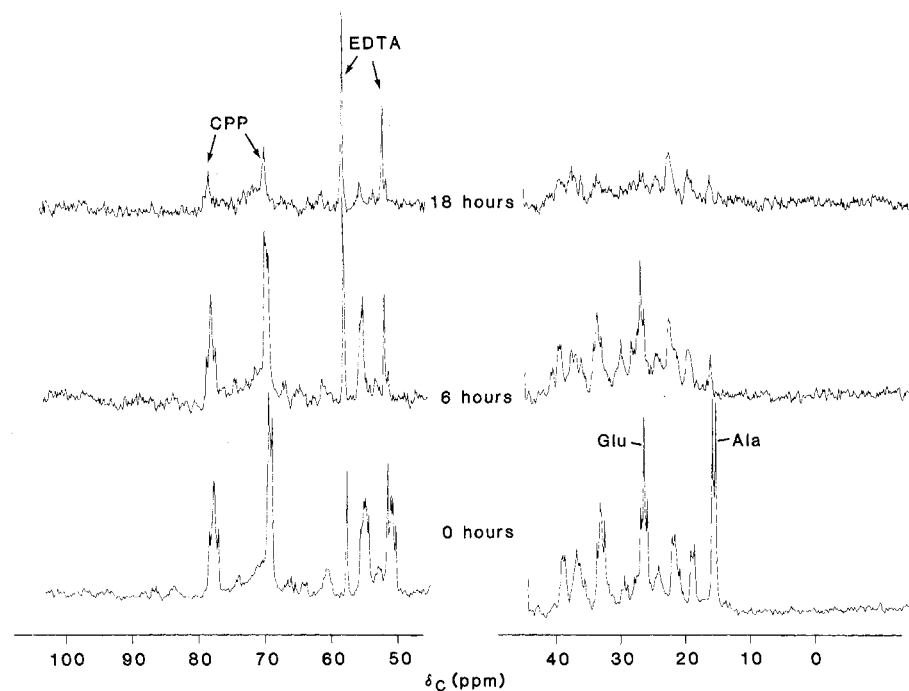


Fig. 3. ^1H -decoupled ^{13}C NMR spectra (67.9 MHz) of ethanol extracts of *Mb. thermoautotrophicum* fed with $^{13}\text{CO}_2/\text{H}_2$ (1:4 by volume) for 0.5 hour followed with $^{12}\text{CO}_2/\text{H}_2$ (1:4 by volume) for the times given (in hours) in the presence of fluoropyruvate (10 mM). Spectra were obtained with the parameters outlined in Fig. 1.

CO_2 . At higher concentrations it also inhibits methanogenesis. Thus it could be expected that, in a feeding experiment with $[1,2-^{13}\text{C}_2]\text{acetate}$ in the presence of propyl iodide (100 μM), CPP would be produced but exchange of bound ^{13}CO with $^{12}\text{CO}_2$ would be unaffected. Figure 2C shows that C-2 of CPP was largely unaffected except that ^{13}C incorporation was lower, whereas the sharp central doublets at C-3 reflect a much larger quantity of ^{13}C next to ^{12}C than in the experiment without inhibitor. Thus more back flux of acetate to C₁ units occurs before it is eventually fixed into CPP. Since this concentration of propyl iodide to some extent affects methanogenesis [and hence the amount of adenosine triphosphate (ATP) available for cellular reactions], the large back flux can be explained as a decrease in the forward flux of acetate into CPP. Therefore, proportionately more scrambling occurs.

In view of the results obtained with these two known inhibitors, we decided to examine the effect of fluoropyruvate on CPP biosynthesis. Fluoropyruvate competitively inhibits pyruvate decarboxylase in *Escherichia coli* (22). It has also been found to inactivate purified pyruvate synthase from *Mb. thermoautotrophicum* in a time-dependent fashion when the enzyme is assayed in the reverse direction (23). The action of fluoropyruvate in this instance is not understood, but there is a precedent for fluoropyruvate

alkylation of free thiol groups with concomitant loss of hydrogen fluoride (24).

Since the purified pyruvate synthase has not been shown to be active in the forward direction, it is cogent to ask how pyruvate may be synthesized in these cells. If fluoropyruvate inhibits the enzyme in vivo, ^{13}C -labeling of CPP should be dramatically reduced, and C₂ units should accumulate. In cells exposed to 10 mM fluoropyruvate, the level of ^{13}C incorporated into CPP from a $^{13}\text{CO}_2$ -pulse- $^{12}\text{CO}_2$ -chase was reduced, and the level of ^{13}C -acetate was not increased (Fig. 3). However, ^{13}C -labeled glutamate (28.9 ppm) and alanine (17.7 ppm) accumulated, and this implies that pyruvate synthase was not being inhibited. Scrambling of CPP derived from $[1,2-^{13}\text{C}_2]\text{acetate}$ was enhanced in the presence of fluoropyruvate (Fig. 2B), similar to the effects with propyl iodide. This was confirmed when cells exposed to fluoropyruvate and $^{13}\text{CO}_2$ for 2 hours exhibited (Fig. 2E) a double doublet for C-3 attributable to promotion of the exchange of C-2 with $^{13}\text{CO}_2$. C-2 showed a sextet of doublets, reflecting the appreciable quantity of ^{12}C at C-3 (from residual $^{12}\text{CO}_2$) and ^{13}C at C-1. The residual ^{12}C at C-2 was exchanged with $^{13}\text{CO}_2$, whereas at C-3 the ^{12}C remained.

A novel CO_2 fixation pathway for methanogens has thus been demonstrated by ^{13}C NMR. The reversibility of CO dehydrogenase has been shown in vivo by the specific

exchange of C-1 of $[^{13}\text{C}_2]\text{acetate}$ with $^{12}\text{CO}_2$ before its incorporation into CPP. The observation that $[^{13}\text{C}_2]\text{pyruvate}$ also undergoes the same exchange reaction implies either that pyruvate synthase, which has been said (25) to operate only in the direction of pyruvate formation, is reversible or that another pyruvate decarboxylation enzyme is operating in vivo. Cyanide inhibits CO dehydrogenase, and propyl iodide evidently inhibits the transfer of a methyl group from methylpterin to a methyl corrinoid (probably through alkylation of the corrinoid cobalt) because, although methanogenesis is not affected by propyl iodide, cell growth is inhibited. Since the exchange reaction with $^{12}\text{CO}_2$ appears to have been promoted, the methyl group must be kinetically sequestered on the corrinoid enzyme for resynthesis of ^{13}C -diluted acetate. It is also conceivable that propyl iodide alkylates a site on CO dehydrogenase, since it has been recently proposed that this enzyme carries out the assembly of acetyl CoA in acetogenic bacteria (14). Indeed this might offer an alternative explanation for the promotion of the exchange reaction in the presence of propyl iodide.

One of the most promising aspects of the ^{13}C isotopic dilution approach is the possibility for screening inhibitors of carbon fixation in vitro for their effect in vivo. For example fluoropyruvate, an inhibitor of cell growth, does not act in vivo by inhibiting pyruvate synthase, since ^{13}C -labeled metabolic products of pyruvate (CPP, glutamate, and alanine) were detected. Instead, isotopic exchange of acetate carbons (and hence CPP carbons) are accelerated, suggesting that fluoropyruvate affects methanogenesis or the C₁ → C₂ condensation reaction.

REFERENCES AND NOTES

1. G. E. Fox *et al.*, *Science* **209**, 457 (1980).
2. G. Fuchs, E. Stupperich, R. K. Thauer, *Arch. Microbiol.* **117**, 61 (1978).
3. G. Fuchs and E. Stupperich, *ibid.* **127**, 267 (1980).
4. E. Stupperich and G. Fuchs, *ibid.* **130**, 294 (1981).
5. ———, *ibid.* **139**, 8 (1984).
6. M. Calvin, *Science* **135**, 879 (1962).
7. M. C. W. Evans, B. B. Buchanan, D. I. Arnon, *Proc. Natl. Acad. Sci. U.S.A.* **55**, 928 (1966).
8. C. T. Taylor, D. P. Kelly, S. J. Pirt, in *Microbial Production and Utilization of Gases (H_2 , CH_4 , CO)*, H. G. Schlegel, G. Gottschalk, N. Pfennig, Eds. (Akademie der Wissenschaften zu Göttingen, East Goltze, 1976), pp. 173–180.
9. J. G. Zeikus, G. Fuchs, W. Kenealy, R. K. Thauer, *J. Bacteriol.* **132**, 604 (1977); L. Daniels and J. G. Zeikus, *ibid.* **136**, 75 (1978); G. Fuchs and E. Stupperich, *Arch. Microbiol.* **118**, 121 (1978).
10. M. Rühlemann, K. Ziegler, E. Stupperich, G. Fuchs, *Arch. Microbiol.* **141**, 399 (1985).
11. S. Kanodia and M. F. Roberts, *Proc. Natl. Acad. Sci. U.S.A.* **80**, 5217 (1983).
12. J. N. S. Evans, C. J. Tolman, S. Kanodia, M. F. Roberts, *Biochemistry* **24**, 5693 (1985).
13. S.-I. Hu, H. L. Drake, H. G. Wood, *J. Bacteriol.* **149**, 440 (1982); E. Pezacka and H. G. Wood, *Proc. Natl. Acad. Sci. U.S.A.* **81**, 6261 (1984).

14. S. W. Ragsdale and H. G. Wood, *J. Biol. Chem.* **260**, 3970 (1985).
15. W. R. Kenealy and J. G. Zeikus, *J. Bacteriol.* **151**, 932 (1982); E. Stupperich, K. E. Hammel, G. Fuchs, R. K. Thauer, *FEBS Lett.* **152**, 21 (1983); G. Diekert and M. Ritter, *FEMS Microbiol. Lett.* **17**, 299 (1983).
16. G. Diekert, M. Hansch, R. Conrad, *Arch. Microbiol.* **138**, 224 (1984).
17. B. Eikmanns, G. Fuchs, R. K. Thauer, *Eur. J. Biochem.* **146**, 149 (1985).
18. P. van Beelen *et al.*, *ibid.* **138**, 563 (1984).
19. R. K. Thauer, G. Fuchs, B. Käufer, V. Schnitker, *ibid.* **45**, 343 (1974); L. Daniels, G. Fuchs, R. K. Thauer, J. G. Zeikus, *J. Bacteriol.* **132**, 118 (1977); G. B. Diekert and R. K. Thauer, *ibid.* **136**, 597 (1978).
20. W. Kenealy and J. G. Zeikus, *J. Bacteriol.* **146**, 133 (1981).
21. U. Holder, D.-E. Schmidt, E. Stupperich, G. Fuchs, *Arch. Microbiol.* **141**, 229 (1985).
22. H. Bisswanger, *J. Biol. Chem.* **256**, 815 (1981).
23. D. J. Livingston and C. T. Walsh, personal communication.
24. Y. Avi-Dor and J. Mager, *J. Biol. Chem.* **222**, 249 (1956).
25. K. Jansen, E. Stupperich, G. Fuchs, *Arch. Microbiol.* **132**, 355 (1982).
26. Supported by the Basic Research Division of the Gas Research Institute (contract 5083-260-0867). We thank W. W. Bachovchin for extensive use of his Bruker AM-400 WB NMR spectrometer. Other NMR spectroscopy was carried out at the Francis Bitter National Magnet Laboratory, Massachusetts Institute of Technology (supported by NIH grant RR 00995 and NSF contract C-670).

30 July 1985; accepted 21 October 1985

Genetic Control of Melatonin Synthesis in the Pineal Gland of the Mouse

SHIZUFUMI EBIHARA, THEODORE MARKS, DAVID J. HUDSON, MICHAEL MENAKER*

Pineal melatonin may play an important role in regulation of vertebrate circadian rhythms and in human affective disorders. In some mammals, such as hamsters and sheep, melatonin is involved in photoperiodic time measurement and in control of reproduction. Although wild mice (*Mus domesticus*) and some wild-derived inbred strains of mice have melatonin in their pineal glands, several inbred strains of laboratory mice (for example, C57BL/6J) were found not to have detectable melatonin in their pineal glands. Genetic analysis suggests that melatonin deficiency in C57BL/6J mice results from mutations in two independently segregating, autosomal recessive genes. Synthesis of melatonin from serotonin in the pineal gland requires the enzymes *N*-acetyltransferase (NAT) and hydroxyindole-*O*-methyltransferase (HIOMT). Pineal glands from C57BL/6J mice have neither NAT nor HIOMT activity. These results suggest that the two genes involved in melatonin deficiency are responsible for the absence of normal NAT and HIOMT enzyme activity.

MELATONIN IS SYNTHESIZED IN the pineal gland from serotonin by a well-known pathway: serotonin is first acetylated to form *N*-acetylserotonin (NAS) by the enzyme *N*-acetyltransferase (NAT), and then NAS is methylated by the enzyme hydroxyindole-*O*-methyltransferase (HIOMT) to form melatonin. NAT activity is cyclic, with high levels at night and lower levels in the daytime (1). This cyclic modulation of NAT activity level is under the control of a circadian pacemaker, which in mammals includes the suprachiasmatic nucleus (2). HIOMT activity is nearly constant throughout the day. Rhythmic NAT activity results in robustly rhythmic melatonin synthesis (1). All vertebrate species so far examined show a daily rhythm of pineal melatonin content (1, 3). We report here that some domesticated inbred

strains of mice (for example, C57BL/6J) have no pineal melatonin at any time of day or night, whereas wild mice of the same species (*Mus domesticus*) synthesize melatonin with normal rhythmicity. Our data

strongly suggest that two independently assorting mutant genes, which affect the activity of NAT and HIOMT, are responsible for the melatonin deficiency in C57BL/6J mice.

We have measured pineal melatonin content in a large number of mice of several different strains (4). These can be divided into three groups: (i) strains that were established as inbred over 40 years ago [C57BL/6J, AKR/J, BALB/c, and NZB/BLN (5)]; (ii) wild-derived strains inbred for less than 30 years [IS/CamEi, SK/CamEi, SF/CamEi, PERU-Atteck/CamEi, and one strain of *Mus castaneus*, the Asian house mouse, CAST/Ei (5, 6)]; and (iii) mice (*Mus domesticus*) trapped in Alberta, Canada, and bred by random mating for about five generations over 5 years in the laboratory of F. Bronson [referred to here as the field-derived strain (FDS)].

We have assayed pineal melatonin content at several times during the day and night (at hours 6, 14, 18, and 22, where hour 0 = lights on and hour 12 = lights off) in male and female mice of the strains in the first group. There was no detectable melatonin in any of these strains at any of the times

Table 1. Segregation of progeny in various types of matings. The expected ratios are calculated on the assumption that two independently segregating genes are responsible for melatonin deficiency in C57BL mice. The lower limit of melatonin detection in our assay is approximately 10 pg per gland (4). It is difficult to accurately estimate very low levels of melatonin, especially given the problems of nonzero cross-reactivity with other compounds such as NAS and variable nonzero blanks. For these reasons we have arbitrarily chosen a measured level below 20 pg per gland to indicate lack of melatonin synthesis. If this level were set at 15 pg, then the χ^2 values would be 13.65 in $F_1 \times C57BL$ and 8.49 in $F_1 \times F_1$. These χ^2 values would allow us to reject the null hypothesis (8). However, χ^2 values obtained if the level were set at 25 or 30 pg would not allow us to reject the null hypothesis. The best χ^2 values for our model are obtained when the threshold level is set at 25 pg ($\chi^2 = 0.317$, $F_1 \times C57BL$; $\chi^2 = 0.423$, $F_1 \times F_1$).

Ratio	No melatonin	Melatonin	χ^2
	<i>F₁ × C57BL</i>		
Observed	60	25	
Expected (of 85 subjects)	63.75	21.25	0.88
	<i>F₁ × F₁</i>		
Observed	21	33	
Expected (of 54 subjects)	23.625	30.375	0.52
	<i>F₁ × FDS</i>		
Observed	0	26	
Expected (of 26 subjects)	0	26	0

S. Ebihara, Department of Animal Physiology, Faculty of Agriculture, Nagoya University, Furo-cho, Chikusa-ku, Nagoya-shi, Aichi 464, Japan.
T. Marks, Case Western Reserve University, School of Medicine, Cleveland, OH 44106.
D. J. Hudson, Department of Neurobiology and Physiology, Northwestern University, Evanston, IL 60201.
M. Menaker, Institute of Neuroscience, University of Oregon, Eugene, OR 97403.

*To whom reprint requests should be addressed.